Design of a Discrete Element Method Parameter Identification System for the Efficient Excavation of Mining Shovels Based on Excavation Resistance Analysis

Hiroyasu Iwata
Faculty of Science and Engineering, Waseda University, Tokyo, Japan
Email: iwata-lab-submission@list.waseda.jp

Siyuan Yu, Saiya Mizushima, and Shinji Yamamura
Graduate School of Creative Science and Engineering, Waseda University, Tokyo, Japan
Email: yusiyuan0902@fuji.waseda.jp, mizushima318@akane.waseda.jp, ys.bd.1205@gmail.com

***Abstract*—Recently, fluctuations in the cost of labor and prices of natural resources have increased the difficulty of the business environment for mine development. Therefore, it is necessary to improve excavation efficiency using hydraulic excavators. Getting the actual excavation resistance for efficient excavation is challenging. To obtain lower resistance in excavation, we aimed to design a Discrete Element Method (DEM) parameter identification system that can calculate excavation resistance. To validate two calculation models in this system, we used a robot arm, different excavation objects, and a DEM software to compare the resistance between the actual excavation and the simulation. We selected the calculation model more approximate to the actual excavation resistance. Thus, our experiments could prove data similarities between simulation and actual excavation. However, a part of excavation resistance is still not approximated in simulation. Therefore, we conducted experiments using steel balls to identify the relationship between the physical properties of excavation objects and the calculated resistance. We obtained conclusions on making calculated resistance more approximate to actual excavation resistance by adjusting the properties.**

***Index Terms*—discrete element method, physical properties excavation resistance, adjustable parameter, parameter identification, excavation trajectories**

I. Introduction

A. Research Background

In recent years, the business environment for mine development has become increasingly difficult due to fluctuations in the cost of labor and natural resources. Consequently, it is need to improve efficiency and reduce fuel consumption. In this study, we aim to improve excavation efficiency by designing a parament idendification system.

Excavation efficiency is based on the operator's experience. Thus, excavation in inappropriate or motionless trajectories could go too deep. Understanding the excavation resistance could help in assessing an operator's skill and assist in correcting the trajectory, thereby improving excavation efficiency and stacking. However, due to the harsh environment of a mine site, directly measuring excavation resistance using load cells is challenging. It is also difficult to calculate the excavation resistance in various soil types, terrains, and trajectories using only available data such as each joint's angle and cylinder pressure. To solve these problems, the Discrete Element Method (DEM) is effective for calculating the excavation resistance [1]-[3]. This is because DEM has a high reproducibility advantage when repeatedly excavating the terrain.

It is desirable to measure the simulation parameters in the field. However, the physical properties of the excavation object are not constant at the mine site.

Since mine sites are harsh environments, it is necessary to use special equipment such as hardness testing machines to measure the physical properties. There have been other studies on excavation resistance analysis of mining shovels, but it is unclear how to adjust the parameters for different soil types when applying the method to different soil types.

Therefore, if the DEM parameters can be determined based on the excavation resistance measured by excavating on a simple trajectory, it will be possible to apply the method to actual mining sites. Based on the above hypothetical configuration, we propose the following system.

1) Using a simple excavation trajectory at the mine site, the resistance generated by the actual mining shovel is measured and accumulated from

Manuscript received December 21, 2021; revised January 20, 2022.

doi: 10.18178/ijmerr.11.5.304-310

cylinder pressure and hand trajectory before operation.

2) A DEM simulation is used to reproduce the excavation described in 1), and the parameters are adjusted so that the resistance of each excavation object is the same as the actual measured value.
3) Excavation is conducted at the mine site using the soil and trajectory used in 1), and the DEM parameters that best approximate the resistance generated are determined.
4) Using the parameters determined in the DEM simulation, various terrains and trajectories at the mine site are reproduced, and the resistance caused by the actual excavation is calculated from the trajectory of the bucket's tip.

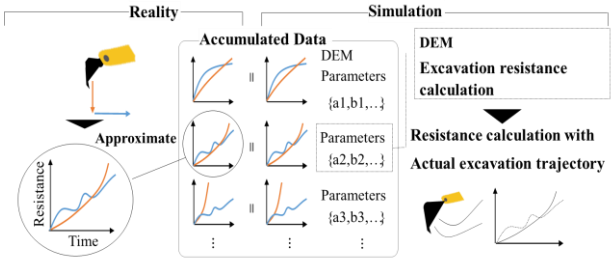

Figure 1. Overview of the proposed system.

As shown in Fig. 1, we designed a system to determine the DEM parameters from the excavation resistance of a simple excavation. This study aims to verify the validity of the proposed system by using a robot arm as the scale model of a hydraulic excavator considering the ease of data acquisition.

B. Prior Research

The DEM was introduced by Cundall in 1971 [4], [5] with the aim of applying it to rock mechanics. As shown in Fig. 2, DEM is used to analyze the behavior of an object by modeling it as a sphere and solving the equation of motion for each time step of the interaction between particles. The equations of motion are solved at each time step, where the impingement distance is the displacement, to reproduce the behavior of fine granular materials.

In the DEM, the behavior differs greatly depending on the model to be applied. To reproduce the actual behavior accurately, models that consider the rolling resistance and interparticle adhesion forces have been devised. Furthermore, it is important to set the parameters to reproduce the behavior more accurately.

Many analyses of excavation resistance of hydraulic excavators using the DEM have been made in [6]–[12]. Yoshida *et al.* [11] examined the difference in excavation efficiency by varying the DEM parameter values (friction coefficient, damping coefficient).

Hirano *et al.* [12] devised an automatic excavation algorithm based on DEM analysis and investigated the excavation efficiency in different trajectories.

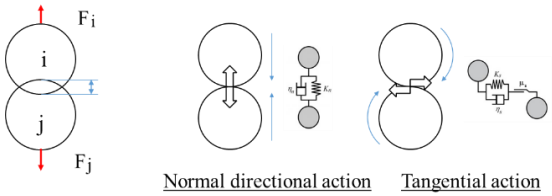

Figure 2. Behavior of the discrete element method.

However, no research aims to reproduce the most suitable behavior and resistance for each excavation.

Our proposed system aims to adjust the DEM parameters based on the data obtained from the excavator. No similar research has been conducted.

II. Validation of the DEM Model

A. Experimental Environment

In this study, an excavation environment using a robot arm is used for ease of data acquisition. The robot arm is DENSO VS060. As shown in Fig. 3, A jig, force sensor (ATI-Mini45), and bucket is attached to the end of the arm.

The jig and bucket were fabricated with a three-dimensional printer.

To calculate the excavation resistance using the DEM, the DEM simulation software "LIGGGHTS" by DCS Computing, an open-source software, was used. The simulation was composed by scripting the scene with this software.

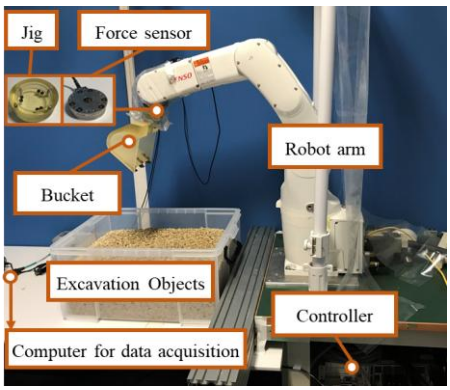

Figure 3. Excavation environment by robot arm.

In LIGGGHTS, each voigt model coefficient is determined by Hooke's law based on various parameters.

In this research, the moments around the bucket's center of rotation are compared with the values measured by the force sensors and the values calculated by the DEM simulation. Therefore, it is necessary to evaluate whether the resistance is reasonably reproduced in the simulation. The Euclidean norm is calculated by considering the difference between each measurement's measured and calculated values as a distance. The smaller the Euclidean norm, the smaller the difference between the measured and calculated values.

B. Excavation Test in the Robot Arm Environment

The excavation resistance was measured with a force sensor attached to the robot arm. The trajectory of the arm used in the test mimicked the actual excavation trajectory. The constructed arm trajectory was evaluated as the correct data. As shown in Fig. 4 and Table I, a trajectory close to the actual excavation trajectory was determined based on the average hand trajectory [13], [14] obtained when an operator with more than 10 years of excavator operation experience excavated a flat surface.

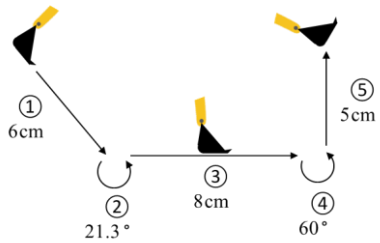

Figure 4. Actual excavation trajectory.

TABLE I. VELOCITY AND ACCELERATION OF EACH PHASE OF THE ACTUAL EXCAVATION TRAJECTORY

No.	Trajectories	velocity (cm/s)	Angular velocity (deg/s)
1	Penetration	5.03	—
2	Rotation	—	17.93
3	Pulling	4.63	—
4	Rotation	—	20.05
5	Lifting	9.15	—

The actual excavation trajectories were used to excavate several different objects. The three objects used in the excavation tests are shown in Fig. 5, and each object's measured physical properties are shown in Table II.

Figure 5. Objects (A, B, C from right).

TABLE II. PHYSICAL PROPETIES OF OBJECT A, B AND C

Objects	Drain size (mm)	Density (kg/m^3)
Object A	10–14	2520
Object B	3–12	2652
Object C	1–3	2310

The excavation object was flattened with a flat plate after each excavation.

The excavation's initial position was set where the toe touched the ground surface. Each excavation's resistance is shown in Fig. 6. These results show that object A has the highest excavation resistance.

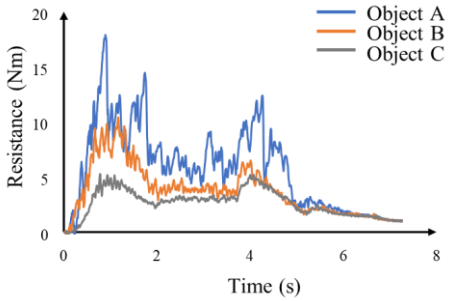

Figure 6. Each object's resistance measured by the excavation trajectory.

C. Validation with the Basic Model

In the simulation, we use the voigt model, the most basic model that does not consider the rolling resistance and interparticle adhesion force. Table III shows the model's parameters. The value 1 is the parameter that adjusted the coefficients of restitution and friction. The numerical value 2 exhibits the case where the density and Young's modulus is increased simultaneously.

The excavation resistance for numerical value 1 is shown in Fig. 7 and Fig. 8. The excavation resistance for numerical value 2 is shown in Fig. 9. Fig. 10 shows the measured values of the force sensors when the robot arm excavated objects A, B, and C.

TABLE III. LIST OF ADJUSTABLE PARAMETERS FOR THE BASIC MODEL

Parameters	Dimensions	Value 1	Value 2
Young's modulus	Pa	1.0×10^8	2.0×10^8
Poisson's ratio	—	0.3	0.3
Coefficient of restitution	—	0.3, 0.6	0.6
Coefficient of Friction	—	0.3, 0.6, 0.9	0.9
Characteristic velocity	—	2	2
Drain size	mm	7.5	7.5
Density	kg/m^3	2.5	5000
Time step	s	0.00001	0.00001

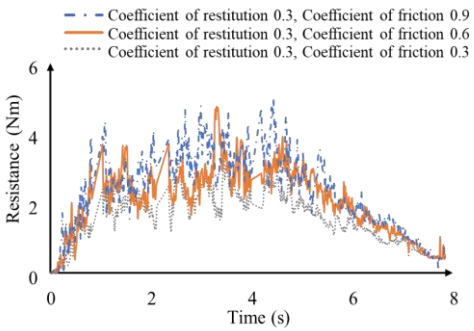

Figure 7. Resistance by DEM in the basic model (Coefficient of restitution 0.3, Coefficient of friction 0.3–0.9).

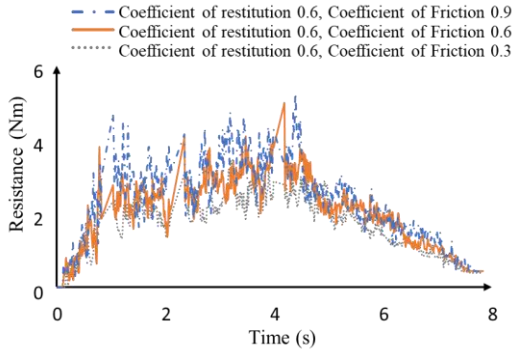

Figure 8. Resistance by DEM in the basic model (Coefficient of restitution 0.6, Coefficient of friction 0.3–0.9).

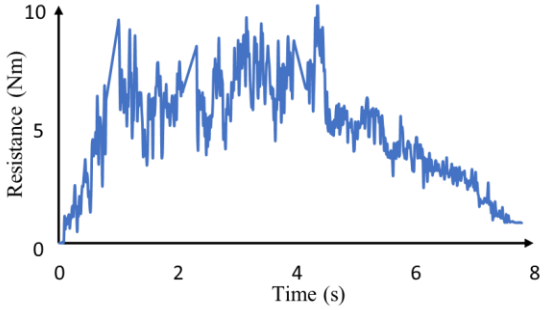

Figure 9. Resistance by DEM (Young's modulus, Density).

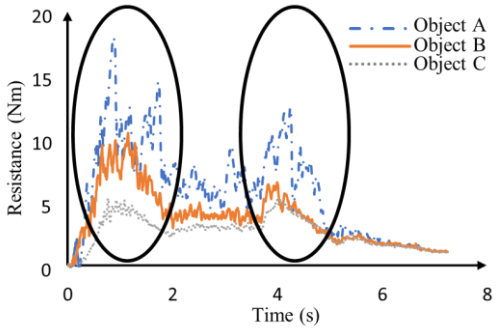

Figure 10. Characteristic waveform of resistance in the actual excavation.

Each excavation's results confirmed that the characteristic peak appeared twice, and the resistance remained low in the valley in-between.

However, unlike Fig. 10, Fig. 7–9 did not show the features mentioned above. The first peak is the penetration and rotation, and the second peak is the rotation of the actual excavation trajectory.

The second peak occurs in the second rotation, i.e., the resistance peak occurs in the rotation. The voigt model used in the simulation can reproduce the translational motion by solving the equations of motion in the normal and tangential directions, respectively.

Although the voigt model used in the simulation can reproduce the translational motion by solving the equations of motion in the normal and tangential directions, it cannot reproduce the rotational motion. In the simulation, the particles are modeled as spheres, so there is little resistance to rotation.

The shape of each excavation is not reproduced simultaneously. Each excavation's shape is irregular and shows strong resistance to rotation. Therefore, the lack of peaks in the simulations is because the particles do not resist rotation.

D. Validation with a Model for Imparting Rolling Resistance

It was difficult to reproduce the resistance pile with the basic model. Therefore, a model with a rolling resistance [15] is used to verify whether the excavation resistance approximates the measured value by adjusting the parameters. The adjusted parameters are shown in Table IV. 48 combinations of each parameter were used in the simulation.

Since the resistances were relatively close, the calculated excavation resistance was used as a reference.

The calculated resistances were relatively close to each other, so the simulated resistances were smoothed using the moving average method by 0.16[s] before and after the simulated resistances to understand the trend of the calculated resistances. Then, the resistance value that most approximated the force sensor's measured value was obtained from the 48 calculated values using the Euclidean norm. Fig. 11 shows the graphs of the most approximate resistance values for objects A, B, and C. The parameters are shown in Table IV, and the parameters for each object when resistance is the most approximated are shown in Table V.

The first peak in object B was not significant, but the second peak and the two peaks in Object A and C were observed. These results suggest that the model with a rolling resistance can reproduce the feature of a real excavation where two large peaks occur in the resistance.

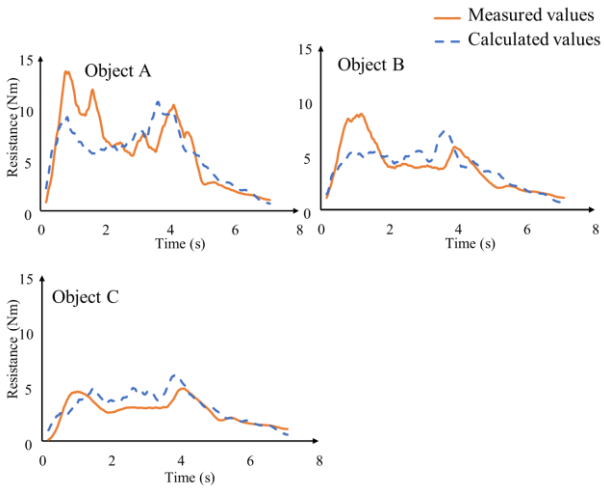

Figure 11. Comparison of calculated values of excavation resistance with the parameters most approximate to each Object.

However, there is an overall misalignment of the waveform. The discrepancy is assumed to be caused by the difference between the simulation and the actual particle shape.

TABLE IV. ADJUSTABLE PARAMETERS IN THE MODEL WITH ROLLING RESISTANCE

Parameters	Dimensions	Value
Young's modulus	Pa	1.5×10^8
Poisson's ratio	—	0.2
Coefficient of restitution	—	0.2
Coefficient of Friction	—	0.3, 0.5, 0.7, 0.9
Coefficients of Rolling Friction	—	0.3, 0.5, 0.7, 0.9
Characteristic velocity	—	2
Drain size	mm	7.5
Density	kg/m^3	1.5, 2.5, 4.0

TABLE V. THE PARAMETER FOR EACH OBJECT WHEN RESISTANCE IS THE MOST APPROXIMATE

Objects	Coefficient of Friction	Coefficients of Rolling Friction	Density (kg/m3)
Object A	0.5	0.9	2.5
Object B	0.3	0.9	2.5
Object C	0.3	0.3	2.5

III. VALIDATION OF THE ADAPTABILITY OF THE PROPOSED METHOD

A. Excavation Experiment on a Simple Excavation Trajectory

The series of flows shown in Fig. 1 is performed to verify the proposed method's adaptability to an excavator. First, an Object X, which has not been used until Chapter 3, is excavated. Based on the excavation resistance, the resistance of the excavator with the closest approximation is determined. The excavation resistance of the actual trajectory is calculated using the parameters adjusted for that excavation and then compared with the measured value of the robot arm. Object X is shown in Fig. 12, and its physical properties are shown in Table VI.

Fig. 13 shows the measured values of the excavation resistance when excavating with the simple trajectory. Table VII shows the measured values of each excavation's resistance and the Euclidean norm of object X's resistance to excavation when it is excavated using the simple trajectory.

From the above, Object X is regarded as object C, and the excavation resistance is calculated using the parameters that best approximate the actual excavation trajectory in object C.

Object X was excavated in a robot arm environment using an actual excavation trajectory. The measured values of the excavation resistance are shown in Fig. 14.

Figure 12. Object X.

TABLE VI. PHYSICAL PROPERTIES OF OBJECT X

Drain size (mm)	Density (kg/m^3)
5–8	1.14

TABLE VII. EUCLIDEAN NORM OF RESISTANCE DURING SIMPLE TRAJECTORY FOR EACH OBJECT AND OBJECT X

Material A	Material B	Material C
89.913	51.267	18.341

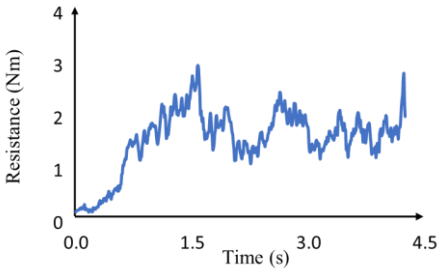

Figure 13. Measured resistance on a simple trajectory (Object X).

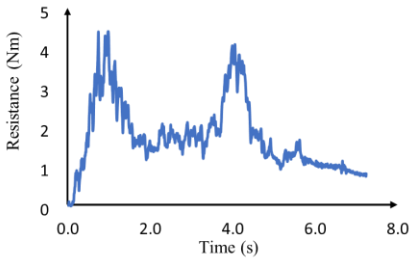

Figure 14. Measured resistance on an actual trajectory (Object X).

B. Approximation on an Actual Excavation Trajectory

The parameters that best approximate object C's resistance during a simple excavation were determined. The calculated values of the actual excavation trajectory using these parameters are compared with object X's excavation resistance during an actual excavation using the robot arm.

Fig. 15 compares the calculated and measured values using object C's actual excavation trajectory. Object C was adjusted from object X's excavation resistance using the simple excavation trajectory to the excavation resistance of Object C that best approximates the resistance of the simple excavation trajectory of each previous excavation.

The calculated values using the DEM are higher than the measured values, but the calculated values could

capture the characteristics of the appearance of peaks. However, As shown in Fig. 16, the actual excavation has a valley in the central part, whereas the calculated value has a peak.

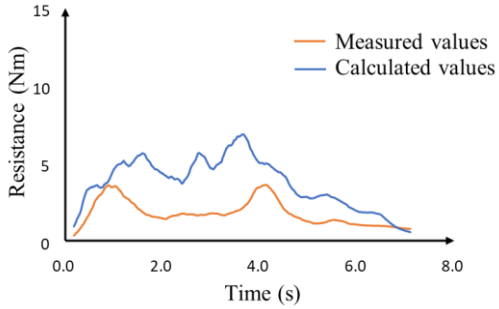

Figure 15. Comparison of actual trajectory with simple excavation identification parameters for Object X.

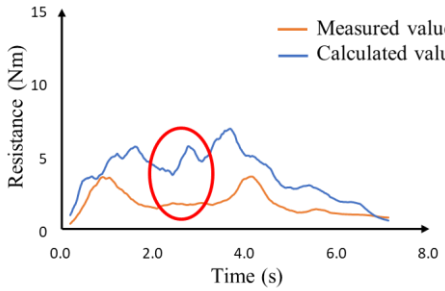

Figure 16. Raising of the central part of the resistance during actual excavation using the identified parameters.

The difference is because the material in the simulation is a perfect sphere and all the particles are of uniform size. However, the actual gravel has an irregular shape, and the particle size varies from one particle to another. Therefore, pulling the bucket forward does not increase the resistance as in the simulation, since small particles escape into the gaps due to the different particle sizes. Therefore, we prepared perfectly spherical steel balls with the same particle size and excavated them. Fig. 17 shows photographs of the drilled steel balls. Table VIII shows the physical properties of the balls. Fig. 18 shows the excavation resistance using the actual excavation trajectory.

Figure 17. 11 mm diameter Steel balls.

TABLE VIII. PHYSICAL PROPERTIES OF STEEL BALLS

Drain size (mm)	11
Density (kg/m^3)	7.82
Young's modulus (Pa)	2.0×10^9

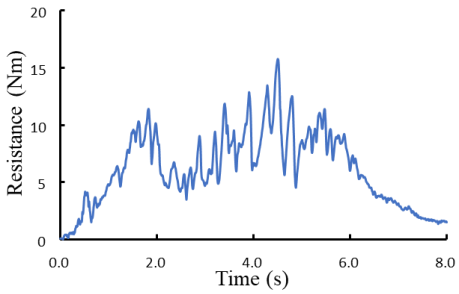

Figure 18. Resistance of 11 mm diameter steel balls using actual trajectory.

Fig. 18 shows that the excavation resistance increases in the central valley. Therefore, to make the simulation closer to the actual excavation, it is necessary to conduct the simulation with a mixture of different particles, i.e., instead of using a high Young's modulus and the density of the steel balls, parameters closer to the actual excavation and far from the physical properties of the balls are used. Using parameters closer to the actual excavated material or further away from the physical properties of the steel balls (lower Young's modulus, lower density), it is possible to reproduce an excavation resistance closer to the actual excavated material, such as an intermediate valley.

Suppose the above does not improve the results. In that case, the excavation resistance can be reasonably calculated by modeling the excavation objects in the simulation as a mixture of particles of different sizes, considering the difference between the actual excavation objects and the ones with the same or different particle size. Furthermore, considering the difference in the shape of the particles, i.e., perfect sphere or irregular shape, we surmise that the excavation resistance can be reasonably calculated by modeling the particles as ellipsoids instead of perfect spheres.

IV. CONCLUSION

We constructed an excavation environment using a robot arm, excavated non-viscous materials such as gravel, and measured the resistance. The comparison between the measured and calculated resistance using the DEM simulation suggests that the rolling resistance model could be applied to reproduce the resistance reasonably well.

A simple trajectory was used to excavate the object without adjusting the parameters beforehand. Consequently, the calculated values were compared with the measured values to evaluate the validity of the system proposed in this study.

The calculated values of excavation resistance when excavating on a real excavation track using the DEM parameters determined by the proposed system were compared with the measured values of excavation resistance by a force sensor when excavating under a robot arm environment on a similar track.

Based on the differences between the two values, steel balls corresponding to particles of uniform size generated

in the DEM simulation environment were examined by excavating in the robot arm environment.

As a future project, a simple excavation trajectory is first listed. Then, the resistance of the actual excavation trajectory will be calculated using the parameters identified based on the resistance during excavation on the trajectory, and the type of simple trajectory required for identifying the DEM parameters will be examined. Finally, the validity of the proposed system will be verified using an actual hydraulic excavator. This will enable further verification of the applicability of the proposed system to mine sites, and various findings and issues in adapting the system to hydraulic excavators will be obtained.

CONFLICT OF INTEREST

The authors declare no conflict of interest.

AUTHOR CONTRIBUTIONS

H. Iwata provided the design of this system. S. Yu and S. Mizushima organized this paper, and translated it to English. S. Yamamura created the excavation environment and did the experiments in this research.

ACKNOWLEDGMENT

We would like to express our sincere gratitude to our collaborators, Mr. Hiraku and Mr. Sugiki from Hitachi Construction Machinery, for their help and advice.

REFERENCES

[1] G. Ishigami, K. Tsuchiya, R. Ishibashi, T. Omura, and S. Ozaki, "High accuracy simulation of construction robot focusing on mutual dynamics between machine and soil-detailed evaluation of excavation mechanics and crawler model and introduction to dynamics simulator," in *Proc. 2018 JSME Conf. on Robotics and Mechatronics*, 2018, pp. 2A1-K02(2).

[2] H. Takahashi, K. Mizukami, and Y. Saito, "Analysis of resistance force during excavation of crushed sediments by power excavator," *Journal of Applied Mechanics*, vol. 6, pp. 603-612, 2003.

[3] A. R. Reece, "The fundamental equation of earth-moving mechanics," in *Proc. Symp. Earthmoving Mach., Instn. Mech. Engrs.*, 1965.

[4] P. A. Cundall, "A computer model for simulating progressive large scale movements in blocky system," in *Proc. Int. Symp. on Rock Fractures*, 1971, pp. II-8.

[5] P. A. Cundall and O. D. L. Strajectory, "A discrete numerical model for granular assemblies," *Geotechnique* vol. 29, no. 1, pp. 47-65, 1979.

[6] C. J. Coetzee, A. H. Basson, and P. A. Vermeer, "Discrete and continuum modelling of excavator bucket filling," *Journal of Terramechanics*, vol. 44, no. 2, pp. 177-186, 2007.

[7] S. Kano, M. Amano, Y. Terasaka, N. Matsumoto, and T. Wada, "Teramechanical simulation using the individual element method," *Komatsu Technical Report*, vol. 49, no. 151, pp. 13-19, 2003.

[8] F. Kanehiro, S. Nakaoka, T. Sugihara, N. Wakisaka, T. Suzuki, G. Ishigami, and S. Ozaki, "ImPACT-TRC simulator study group-simulation of natural phenomena, road surface deformation and excavation," in *Proc. of the 2017 JSME Conf. on Robot. and Mechatron.*, 2017, pp. 2A1-Q12.

[9] S. Uemura and E. Imanishi, "Dynamic simulation of rigid-body and hydraulic drive system considering excavation behavior of soil," *Transactions of the JSME*, vol. 84, no. 861, pp. 17-00468, 2018.

[10] C. J. Coetzee and D. N. J. Els, "The numerical modelling of excavator bucket filling using DEM," *Journal of Terramechanics*, vol. 46, no. 5, pp. 217-227, 2009.

[11] T. Yoshida, "A study on automation of hydraulic excavator by simulation," Ph.D Thesis, Doshisha University, Tokyo, Japan, 2013.

[12] T. Hirano, T. Yoshida, N. Tsujiuchi, A. Itoh, F. Kuratani, T. Tateishi, T. Atsumi, and H. Ando, "Investigation of control parameters for soil parameters in automatic excavation of hydraulic excavators," in *Proc. 61st Japan Joint Automatic Control Conf.*, pp. 1263-1270, 2018.

[13] M. Yamai, T. Kawahara, M. Itoh, and Y. Nakata, "Proposal of a liquid crosslinking force model considering no-slip effect," *Journal of the Society of Powder Technology*, vol. 54, no. 42, pp. 782-788, 2017.

[14] Y. Nakagawa, "DEM analysis of adhesive earth excavation work using bulldozer blade," *Osaka University Industrial Association Techno Net*, vol. 561, pp. 14-18, 2013.

[15] J. Ai, J. F. Chen, J. M. Rotter, and J. Y. Ooi, "Assessment of rolling resistance models in discrete element simulations," *Powder Technology*, vol. 206, no. 3, pp. 269-282, 2011.

Hiroyasu Iwata is a professor in Faculty of Science and Engineering, Waseda University, Japan.
His research interests include rehabilitation assistive RT, medical care RT, Support System for Teleoperators of Disaster Response Robots and Application of Electronic Nanosheet.
Professor Hiroyasu is the membership of IEEE, EMBS, JSBR, RSJ, etc.

Siyuan Yu was born in September 1997 in China. He received his Bachelor degree in 2019 in Huaqiao University, China.
He is currently a Master student in IWATA Lab, Waseda University, Japan. His current research interests include construction machinery, efficient excavation of mining shovels and robotics.

Saiya Mizushima was born in March 1996 in Shizuoka, Japan. He entered School of Creative Science and Engineering, Waseda University, Japan in 2016 and received his Bachelor degree in 2020.
He is currently a Master student in IWATA Lab, Waseda University, Japan. His research is mainly about efficient excavation by DEM simulation.

Yamamura Shinji was born in December 1994 in Japan. He received his bachelor degree in 2016 in School of Creative Science and Engineering, Waseda University, Japan and master degree in 2018 in Graduate School of Creative Science and Engineering, Waseda University, Japan.
His research interests were mainly about construction machinery.